Two-Terminal Millimeter-Wave Sources

Heribert Eisele and George I. Haddad, *Life Fellow, IEEE*

***Abstract*— Basic principles of operation, fundamental power-generation capabilities, and fabrication technologies are reviewed for three groups of two-terminal devices, i.e., resonant-tunneling diodes (RTD's), transferred-electron devices (TED's), and transit-time diodes. The paper focuses on devices for frequencies above 30 GHz, and an overview of recent research in this area and of various state-of-the-art laboratory results is given. As an outlook, the potential of some new material systems for high-power devices is discussed.**

***Index Terms*— Etching, gallium compounds, Gunn devices, IMPATT diodes, indium compounds, millimeter-wave devices, millimeter-wave generation, millimeter-wave oscillators, oscillator noise, phase noise, silicon, silicon compounds, submillimeter-wave devices, submillimeter-wave generation, submillimeter-wave oscillators.**

I. Introduction

DESPITE the rapid progress in the upper frequency limits and RF power levels of three-terminal devices [1]–[5], two representatives of two-terminal devices, i.e., Gunn devices and impact avalanche transit time (IMPATT) diodes, together with vacuum tubes, still play an important role in many system applications. Three-terminal devices have almost entirely superseded two-terminal devices in low-noise preamplifiers, up to millimeter-wave frequencies. This paper will mainly focus on oscillators and will give an overview of resonant-tunneling diodes (RTD's), Gunn or transferred-electron devices (TED's), and transit-time diodes, as well as their fundamental power-generation capabilities at millimeter-wave frequencies. Various power-combining techniques were utilized to increase the available RF output power, and examples will be presented for each of the discussed two-terminal devices.

II. General Technology

Selective etching technologies with the benefits of, e.g., well defined and highly reproducible mechanical dimensions of the device mesa and contact structures, are employed in the fabrication of most of the present state-of-the-art two-terminal devices. The flowchart of Fig. 1 serves as an example and illustrates the fabrication steps for GaAs IMPATT or tunnel injection transit-time (TUNNETT) diodes on integral heat sinks [6], [7]. More detailed descriptions of various fabrication technologies for devices in the Si-, GaAs-, and InP-material systems or references to them are given in [6]–[11]. In the first step, as shown in Fig. 1, the metallization for the p-ohmic contact (Ti/Pt/Au) is evaporated or sputtered onto the surface. A thick gold layer is then electroplated onto this metallization to form the integral heat sink. The sample is mounted on a carrier to provide additional mechanical support and to protect the heat sink from etchants during the subsequent fabrication steps. The substrate is removed in a well-known selective etchant of $H_2O_2:NH_4OH$ 1:19 [12], [13], which does not significantly attack the $Ga_xAl_{1-x}As$ stop-etch layer if $x > 0.4$.

Ohmic contacts are more difficult to form on $Ga_xAl_{1-x}As$ than on GaAs. Therefore, this $Ga_xAl_{1-x}As$ layer is selectively removed in a solution of HF, which does not attack GaAs. A photolithography step defines the openings on this heavily n^+-doped GaAs layer, where the standard metallization (Ni/Ge/Au/Ti/Au) for the n-ohmic contacts is deposited. Excess metal outside the contacts is lifted off with the photoresist and, using another photolithography step, each contact is selectively electroplated with several microns of gold to form a good bonding pad. The contact pad then acts as a mask when the mesa of the diode is etched in a nonselective etchant. After the sample has been removed from the carrier, the contacts are annealed, and the sample is diced into individual diodes. Diodes are then mounted in packages for appropriate RF circuits.

Proper thermal management is one of the most critical issues in high-power two-terminal devices, and high-performance devices for reliable long-term operation are generally mounted on diamond heat sinks [8]–[11], [13]–[18]. Typically, heat-flow resistances of mesa-type devices on diamond heat sinks are at least a factor of two lower than those of devices on integral heat sinks.

III. RTD's

RTD's utilize the distinctive properties of the carrier transport across a double heterojunction barrier [19], as illustrated in Fig. 2, for the InGaAs/InAlAs and InGaAs/AlAs material systems. If, under bias, one of the discrete energy levels in the quantum well between the barriers lines up with the conduction band outside, a large (resonant-) tunneling current of electrons will flow from the band outside through the barriers [19]. This process causes current–voltage characteristics, as shown in Fig. 2, for the RTD's with high peak-to-valley ratios (PVR's) J_p/J_v in the InAlAs/InGaAs and AlAs/InGaAs material systems. The RTD exhibits a negative differential resistance if biased between the V_p, the voltage for the peak current density J_p, and V_v, the voltage for the valley current density J_v. Since this (resonant-) tunneling process is very fast, this negative resistance exists from dc up to submillimeter-wave frequencies. This very broad-band negative resistance

Manuscript received October 17, 1997; revised March 4, 1998.

The authors are with the Solid-State Electronics Laboratory, Department of Electrical Engineering and Computer Science, University of Michigan, Ann Arbor, MI 48109-2122 USA (e-mail: heribert@engin.umich.edu; gih@eecs.umich.edu).

Publisher Item Identifier S 0018-9480(98)04035-6.

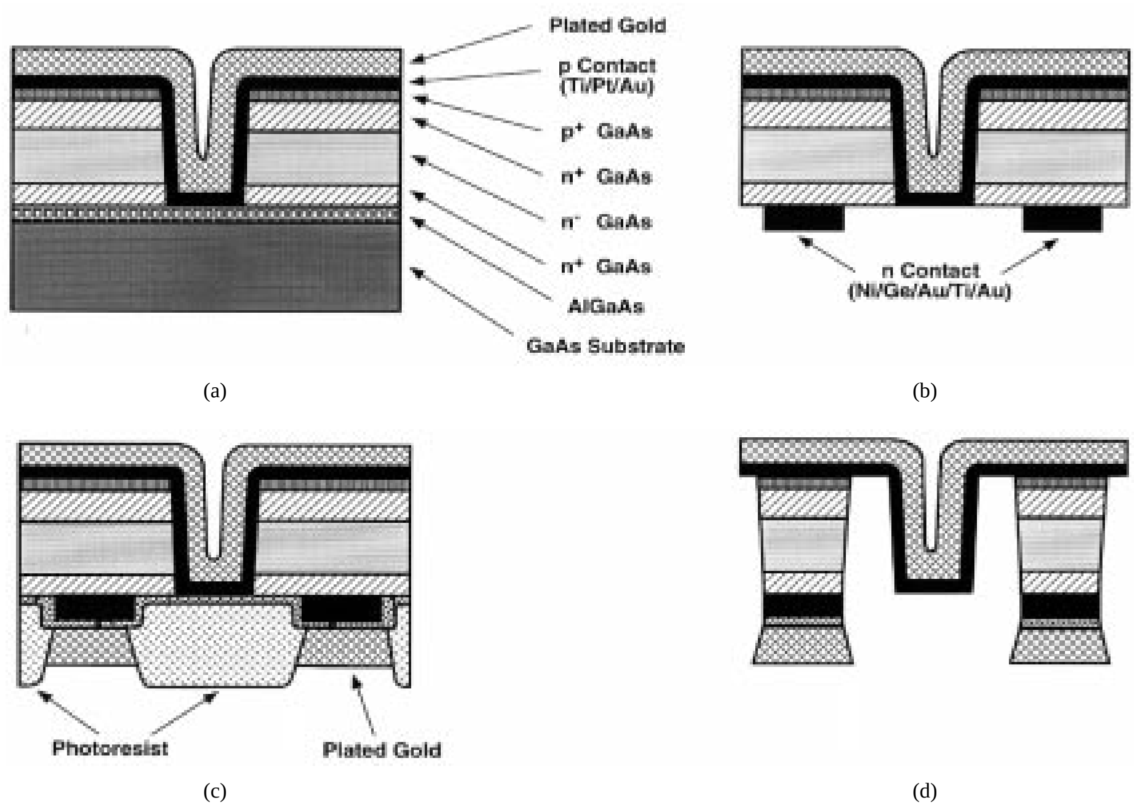

Fig. 1. Flowchart with the fabrication steps for GaAs IMPATT or TUNNETT diodes on integral heat sinks [6], [7]. (a) Island definition, p-ohmic evaporation and gold plating of heat sink to approximately 20 μm. (b) Substrate thinning, stop-etch layer removal, and n-ohmic evaporation. (c) Gold plating of ohmic contacts. (d) Final diodes after mesa etch and annealing.

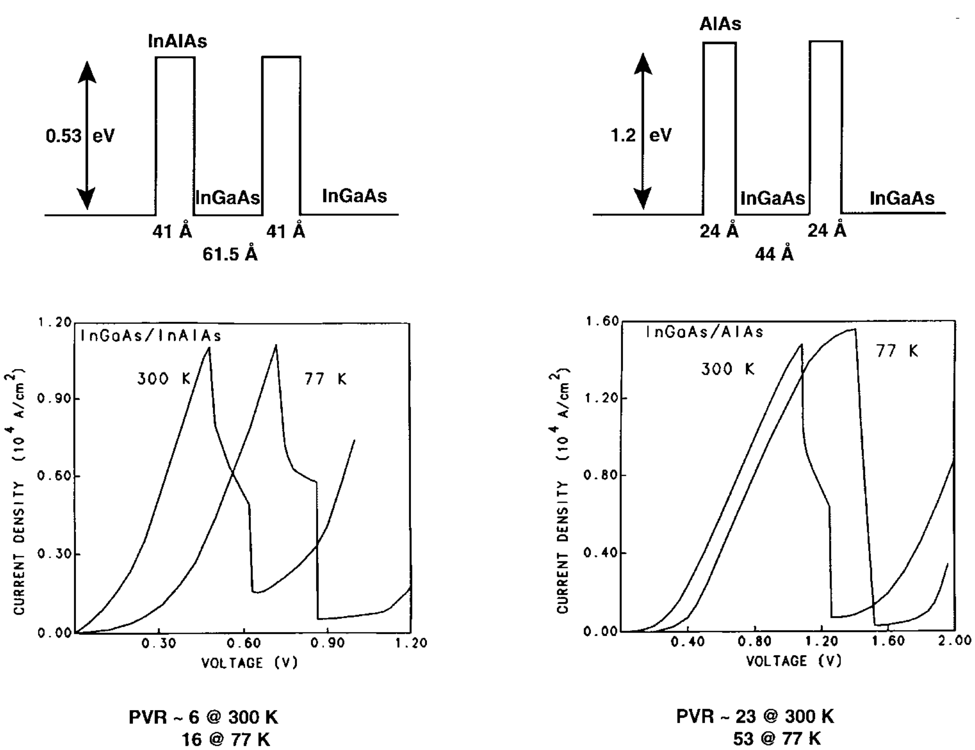

Fig. 2. Conduction band profiles and current–voltage characteristics for lattice-matched InAlAs/InGaAs and strained AlAs/InGaAs RTD's with high PVR's.

easily leads to bias–circuit oscillations, and a simple analysis [6] reveals two conflicting power limitations in these diodes.

A simplified equivalent circuit for an oscillator with a resonant circuit as the load and a series resistance R_s for the combined losses, contact resistances, and so forth is shown in Fig. 3, and includes relevant elements of the bias circuit. Operation in an oscillator at such a high-frequency ω is assumed so that the capacitance (per unit area) C_D of the

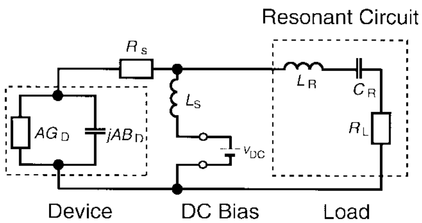

Fig. 3. Simplified equivalent circuit of an oscillator with an RTD connected to a bias circuit and load [6].

depleted region becomes dominant, i.e.,

$$\omega C_D \frac{V_v - V_p}{J_p - J_v} \gg 1. \tag{1}$$

Generally, the smallest load resistance R_L that can be presented to the two-terminal device determines the maximum device area A. In this case, the RF circuit limits the RF output power P_{RF}, and with the specific series resistance $\rho_s = R_s A$

$$P_{\mathrm{RF}} = \frac{1}{8\omega^2 C_D^2} (J_p - J_v)^2 \frac{R_L}{\left(R_L + \frac{\rho_s}{A}\right)^2}. \tag{2}$$

However, to avoid oscillations in the bias circuit, the following much smaller area must be chosen [6]:

$$A = \frac{\rho_s C_D}{L_S} \frac{J_p - J_v}{V_v - V_p} \tag{3}$$

which severely reduces the power to

$$P_{\mathrm{RF}} = \frac{\rho_s C_D}{8L_S} \left[1 + \rho_s \frac{\omega^2 C_D^2 (V_v - V_p)}{J_v - J_p}\right] (V_v - V_p)^2. \tag{4}$$

RTD's in waveguide circuits are, in general, contacted by a whisker [20], and this whisker inductance is a major contribution to L_S (3), (4), which cannot be reduced much.

RTD's for oscillators were realized in the InGaAs/AlAs, GaAs/AlAs, and InAs/AlSb material systems. Oscillation frequencies up to 712 GHz with InAs/AlSb RTD's [20] are the highest achieved to date and exceed those of any other two-terminal (and also three-terminal) devices. As illustrated in Fig. 4, RF power levels are low, although power combining was shown to bring about considerable improvement [21] and, as an example, the RF power of 28 μW was measured at 290 GHz [22]. In this monolithic approach, part of the bias circuitry is integrated and helps reduce L_S. The highest RF power levels of 200 μW at 100 GHz and 50 μW at 205 GHz were reported from InGaAs/AlAs RTD's [23]. Low output power levels, together with the inherent tendency for bias instabilities have, so far, severely limited the use of RTD's in system applications, and only one experiment with an RTD in a receiver system was reported [24].

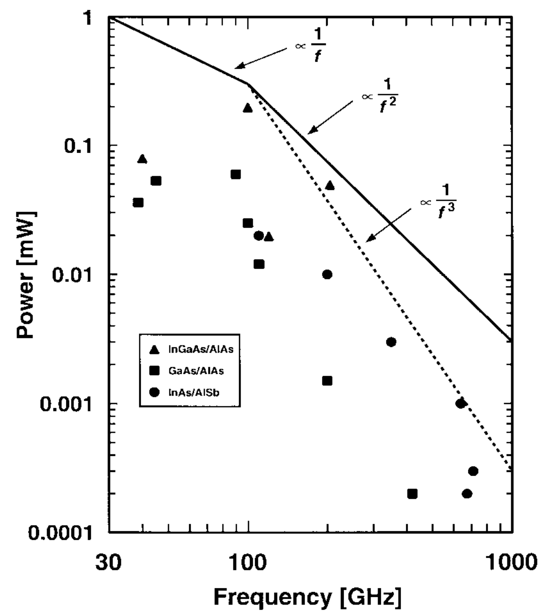

Fig. 4. Published state-of-the-art RF power levels from RTD's in the frequency range of 30–1000 GHz.

IV. TED's

The operation of TED's is based on a specific conduction-band structure with several minima (valleys) that allow an electron transfer from a central valley with low effective mass and high mobility to at least one satellite valley with high effective mass and low mobility. This type of transfer is possible in many compound semiconductor materials [25], but, so far, only GaAs and InP have played a major role. Acceleration–deceleration and energy relaxation times in the range of 0.4–1.5 ps for GaAs and 0.2–0.75 ps for InP [6], [26], [27] govern this intervalley transfer process, cause a so-called "dead zone" in the active region [6], and impose a fundamental frequency limit on Gunn devices. As illustrated in Fig. 5 for a W-band (75–110 GHz) InP Gunn device with a 1.7-μm-long active region, the dead zone can be regarded as an additional series resistance that diminishes the dynamic negative resistance of the device. Current-limiting contacts [14], [26], [27] and heterojunction barriers [28] are examples of experimentally tested approaches to a substantial reduction of this dead zone. The fundamental frequency limit is estimated to be near 100 GHz in GaAs TED's and near 200 GHz in InP TED's [6], [26], [27] and corroborated by experimental results with fundamental-mode operation exceeding 80 GHz in GaAs TED's [16], [28] and exceeding 160 GHz in InP TED's [7], [18]. Due to their excellent noise properties in medium-power oscillators, TED's have found widespread use as local oscillators and drivers for multiplier or amplifier chains in many system applications. Fig. 6 summarizes the state-of-the-art RF power levels from InP and GaAs TED's above 30 GHz. Fundamental-mode operation suffers a sharp decline in the RF performance above approximately 70 GHz, as seen in GaAs TED's, and above approximately 140 GHz, as seen in InP TED's, which presages the above fundamental frequency limits. However, operation in a second-harmonic-mode has been proven to be very effective in extending the useful frequency range of TED's with RF power levels of, e.g., 96 mW at 94 GHz [29] and 7.5 mW at 180 GHz [30].

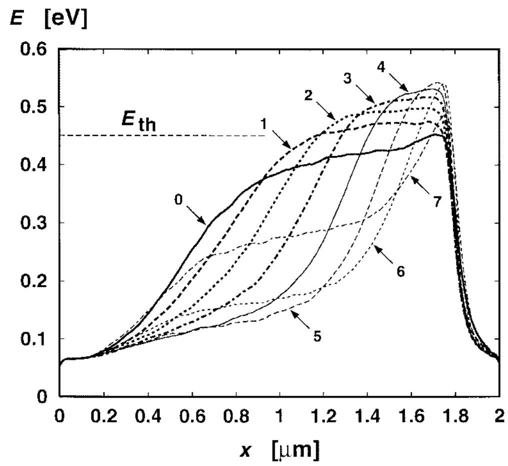

(a)

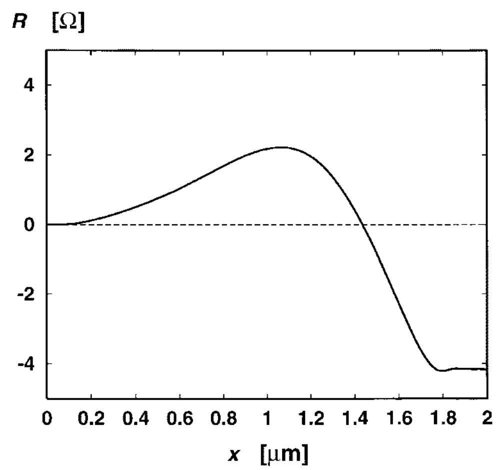

(b)

Fig. 5. (a) Evolution of average electron energy E. (b) Diode resistance R as a function of position x (active region from 0.1 to 1.8 μm): $f = 95$ GHz, $V_{\rm rf} = 1.0$ V, $V_{\rm bias} = 5.0$ V, $I_{\rm bias} = 474$ mA, $T = 500$ K. The graphs in (a) show the electron energy profile at $\omega t = n\pi/4$, $n = 0, \cdots, 7$ during one RF cycle [6].

Various experimental results at millimeter-wave frequencies demonstrated that power combining with Gunn devices (in particular, the fundamental mode) is straightforward and that high combining efficiencies (even exceeding 100%) can be easily obtained up to the highest frequencies [31], [32].

V. Transit-Time Diodes

A confined bunch of carriers is generated in a narrow region (by different means, depending on the type of diode [6], [25]) and its transit through a depleted region induces a current flow in the outer circuit. The phase delay between the RF voltage at the terminals and the induced current results in a dynamic negative resistance and the generation of RF power. IMPATT diodes with significant power levels have been realized with the semiconductor materials Si, GaAs, and InP. Si and GaAs IMPATT diodes are commercially available. Fig. 7 summarizes the state-of-the-art RF power levels from various transit-time diodes. Below 60 GHz, GaAs IMPATT diodes offer higher RF output power and dc-to-RF conversion efficiency than their Si counterparts, whereas only Si IMPATT

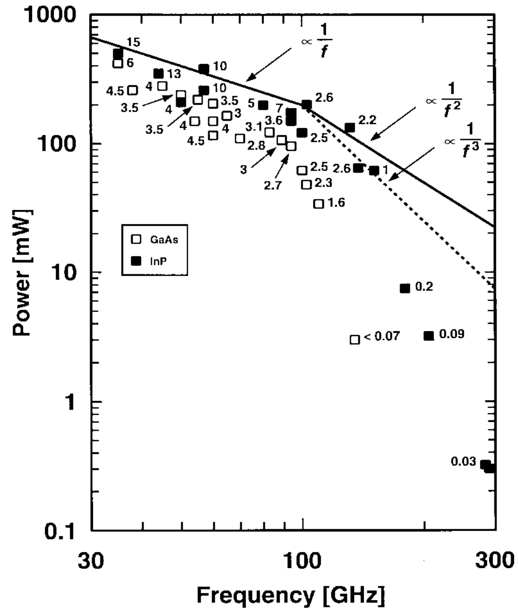

Fig. 6. Published state-of-the-art RF power levels from TED's under continuous wave (CW) operation in the frequency range of 30–300 GHz. Numbers next to the symbols denote dc-to-RF conversion efficiencies in percent.

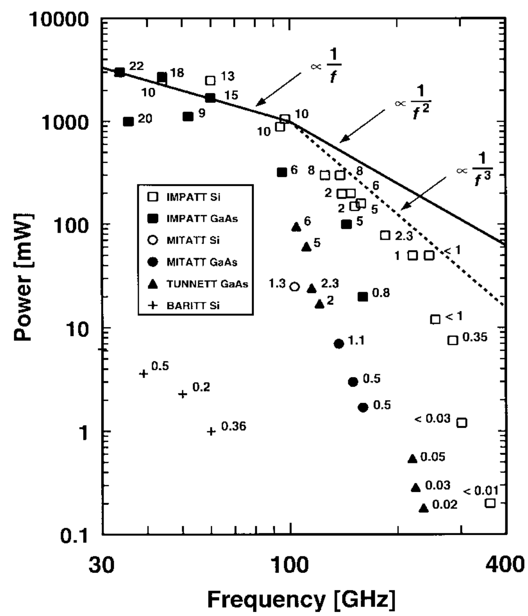

Fig. 7. Published state-of-the-art RF power levels from various transit-time diodes under CW operation in the frequency range of 30–400 GHz. Numbers next to the symbols denote dc-to-RF conversion efficiencies in percent.

diodes reach oscillation frequencies above 300 GHz [33]. Many of the state-of-the-art RF power levels from Si, but also GaAs IMPATT diodes in Fig. 7, were the results of major research and development efforts in the late 1970's and 1980's [14], [15], [33]. Recent research in the area of Si and GaAs IMPATT diodes focuses on refining the state-of-the-art by improving fabrication technologies and by employing advanced growth techniques such as molecular-beam epitaxy (MBE) to implement more complex doping profiles [8], [11], [15], [17], as illustrated in Fig. 8. Such doping profiles increase the available impedance level for the same diode area and

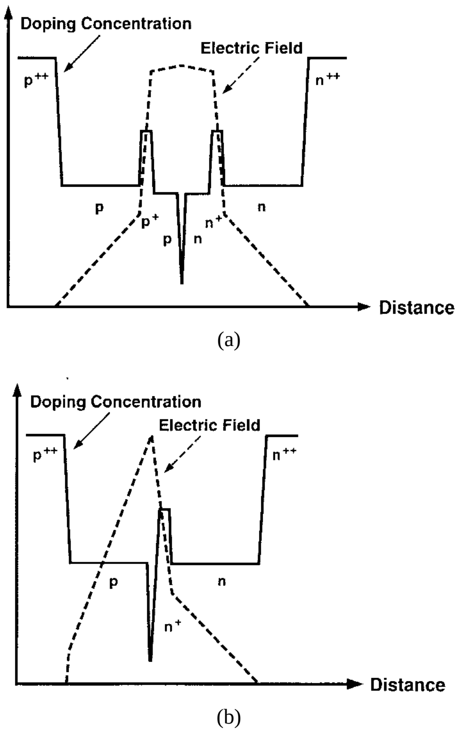

Fig. 8. Schematic doping profiles for high-power high-efficiency double-drift IMPATT diodes. (a) Double-drift Hybrid Read low–high–low. (b) Double-drift Hybrid Read flat–high–low.

improve dc-to-RF conversion efficiency as well as RF output power. Conversely, higher dc-to-RF conversion efficiencies help reduce the dc power consumption and ease the thermal constraints of planar oscillators [34] where most of the heat has to be dissipated into the semiconductor material with a typically much lower thermal conductivity than most metals.

Contrary to RTD's and TED's, IMPATT diodes have also found widespread use in applications where they are driven with pulses. This mode of operation overcomes thermal limits and results in significantly higher peak RF power levels such as 28 W at 35 GHz [14], 42 W at 96 GHz [11], and 5.6 W at 140 GHz [14] from Si IMPATT diodes under short 50–200-ns-long pulses.

Numerous power-combining techniques were extensively investigated and subsequently employed in Si and GaAs IMPATT amplifiers and oscillators. A review of power-combining techniques can be found in [31]. Examples of CW operation are the RF output power of 20 W at 44 GHz for an output stage of 16 Si IMPATT diodes [35] and 5.9–6.5 W at frequencies of 60.5–62.5 GHz for an output stage of eight GaAs IMPATT diodes [36].

VI. New Materials

Considerably higher RF power levels, in pulsed mode in particular, can be expected from transit-time diodes if wide-bandgap materials such as SiC, GaN, and diamond are used. As is well known [25], the RF power generated from a transit-time diode is proportional to the figure of merit $M_p = (\mathcal{E}_c v_s / f)^2$. Table I summarizes relevant material parameters of semiconductors that can play an important role for transit-time diodes. Their power-generation capabilities are compared in terms of M_p relative to Si. However, significant additional efforts are required in the areas of material growth and characterization, as well as doping and processing technologies before the full potential of these wide-bandgap materials can be utilized.

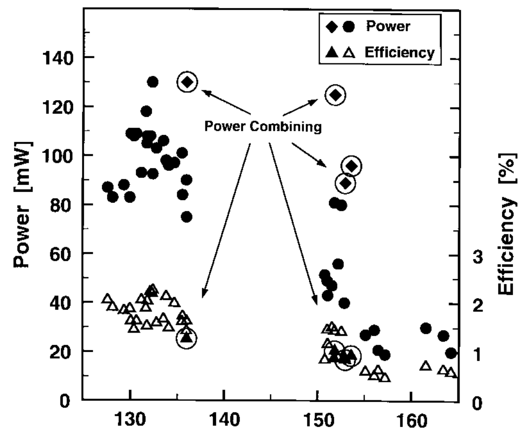

Fig. 9. RF output power and dc-to-RF conversion efficiency versus oscillation frequency for D-band InP Gunn devices fabricated from epitaxial material grown by metal–organic chemical-vapor deposition.

TABLE I
PROPERTIES OF IMPORTANT SEMICONDUCTORS FOR RF POWER GENERATION

	Si	GaAs	InP	6H-SiC (4H-SiC)	GaN	Diamond
Band Gap (eV) (@ 300 K)	1.12	1.42	1.34	3.06 (3.26)	3.39	5.5
Electron mobility (@ 300 K, cm^2/Vs) $\perp$ c-axis, $\parallel$ c-axis	1400	8500	4600	400 (850) 80 (1020)	900	2200
Hole mobility (@ 300 K, cm^2/Vs)	450	400	140	90 (115)	150	1600
Breakdown field $\mathcal{E}_C$ (10^6 V/cm) (@ $N_D \sim 10^{17} cm^3$)	0.61	0.65	0.75	2.5 (2.2)	2	10
Thermal conductivity (W/cmK)	1.25	0.46	0.68	4.9	1.3	20
Sat. electron drift vel. v_s (10^7 cm/s) (@ $\mathcal{E} > 5 \times 10^5$ V/cm)	1	0.6	0.75	2	2.7	2.7
Dielectric constant	11.8	12.8	12.6	9.7	9	5.5
Electronic P_{RF} figure-of-merit relative to Si $(\mathcal{E}_C v_s)^2$	1	0.4	0.9	70	80	2000

VII. Selected Experimental Results

Research at the University of Michigan at Ann Arbor contributed to, or resulted in, several state-of-the-art results from two-terminal devices. RF power levels of more than 200 mW at 103.1 GHz [32] and, as shown in Fig. 9, power levels of more than 130 mW around 132 GHz and more than 80 mW at 152 GHz (with low FM noise measures and very low phase noise) were achieved with InP Gunn devices on diamond heat sinks [18].[1] These RF power levels are the highest reported to date from any Gunn devices and they correspond to dc-to-RF conversion efficiencies exceeding 2.3% between 102–132 GHz. Four results from the first

[1] H. Eisele, unpublished results.

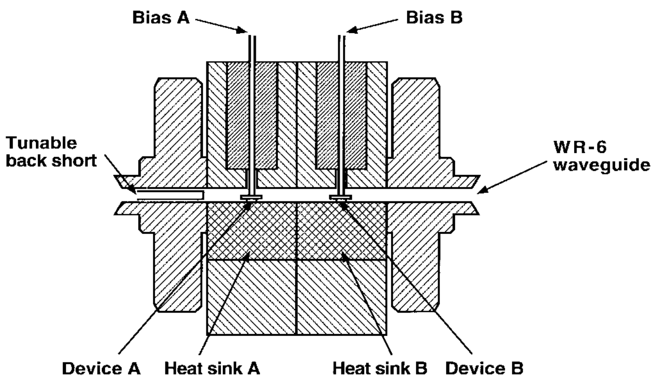

Fig. 10. Schematic of the in-line dual-cavity waveguide circuit for power-combining InP Gunn devices in fundamental-mode operation.

successful demonstration of power combining with D-band (110–170 GHz) Gunn devices [32],[1] are also included in Fig. 9. RF power levels of more than 300 mW at 106 GHz, 130 mW at 136 GHz, and more than 125 mW at 152 GHz were obtained using the in-line dual-waveguide cavity configuration of Fig. 10. Oscillators with these power-combined devices maintain the same excellent phase–noise properties as those with single devices [32], and also retain some of the smooth tuning capabilities [32]. Second-harmonic power extraction from these InP Gunn devices was shown to be possible up to at least 290 GHz [10] and, as examples and preliminary results, RF power levels of more than 0.3 mW at 283 GHz [10] and 2 mW at 223 GHz were demonstrated.[2]

Work has been, and is being, performed in the area of GaAs and InP IMPATT diodes, and InP is emerging as a new potential candidate for high-performance IMPATT diodes [37]. Exemplary results for simple single-drift flat-profile GaAs IMPATT diodes are RF power levels (and corresponding dc-to-RF conversion efficiencies) of 320 mW (7%) at 92 GHz and more than 10 mW (>1.0%) at 140 GHz [38].[1] TUNNETT diodes can compete in RF output power, e.g., 100 $\pm$ 5 mW at 100–107 GHz [9],[1] with GaAs Gunn devices around 100 GHz [29], whereas their dc-to-RF conversion efficiencies, e.g., 5.8%–6.1% at 100–107 GHz [9],[1] are much higher than those of GaAs Gunn devices [29]. Contrary to GaAs Gunn devices [29], these GaAs TUNNETT diodes operate around 100 GHz in the fundamental mode. Since they also exhibit strongly nonlinear properties, second-harmonic power extraction can be utilized [9] and, as preliminary results, yielded RF power levels of approximately 3 mW at 217.6 GHz and more than 2 mW at 234.5 GHz, which correspond to dc-to-RF conversion efficiencies of more than 0.3% and remarkable up-conversion efficiencies of between 6% and more than 10%.[1] As illustrated with the spectrum in Fig. 11 of a free-running oscillator at 217.6 GHz, the excellent phase noise of much lower than -87 dBc/Hz at a frequency off the carrier of 500 kHz, correctly reflects phase noise of much lower than -93 dBc/Hz, which was measured at the fundamental frequency [9],[1] and similar dc bias.

Power-combining efficiencies around 80% and a combined RF power of more than 140 mW at 104 GHz [9] were achieved

[2] H. Eisele and A. Rydberg, unpublished results.

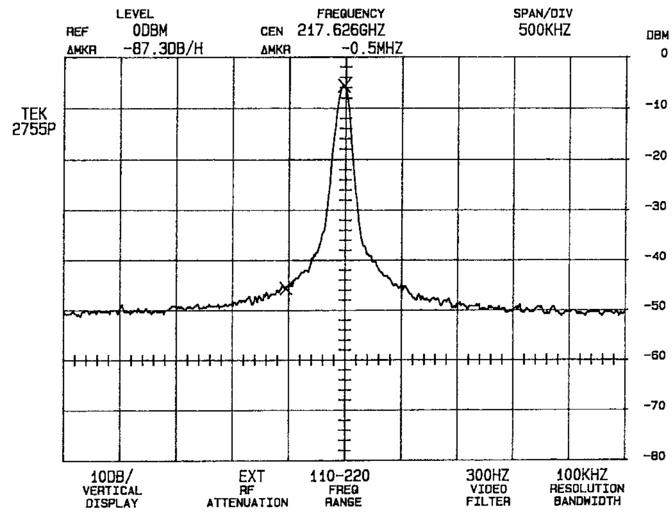

Fig. 11. Spectrum of a W-band TUNNETT diode free-running oscillator in a second-harmonic mode, RF power level 3 mW, center frequency 217.6 GHz, vertical scale 10 dB/div, horizontal scale 500 kHz/div, BW 100 kHz, video BW (VBW) 300 Hz.

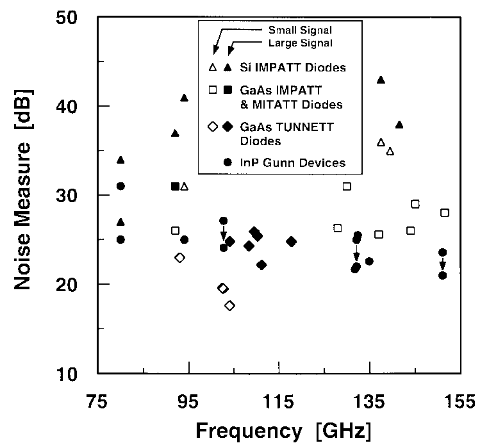

Fig. 12. FM noise measure M of free-running oscillators with transit-time diodes and TED's in the frequency range of 75–155 GHz (published and unpublished results).

with two GaAs TUNNETT diodes, each in a simple in-line dual-cavity configuration [9] similar to Fig. 10. The diodes appeared to be phase-locked readily and without spurious signals when tuned for maximum RF output power. They also demonstrated clean spectra with excellent phase noise properties, as seen in free-running oscillators with one GaAs TUNNETT diode.

Fig. 12 compares the FM noise measure M [39], [40] of free-running oscillators with different transit-time diodes and TED's. This noise measure M is defined as follows:

$$M = \frac{\Delta f_{\rm rms}^2 Q^2}{f_o^2 k T_0 B} P_{\rm RF} \tag{5}$$

where $\Delta f_{\rm rms}$ is the effective frequency modulation, Q the loaded quality factor of the resonant cavity, $P_{\rm RF}$ the RF output power, f_o the oscillation frequency, T_0 the absolute temperature of the RF load, k the Boltzmann constant, and B the measurement bandwidth. In the small-signal case, the oscillators are typically operated under conditions where less than 10% of the maximum available RF power is generated. The lowest FM noise measures (<18 dB) for any oscillator with two-terminal devices were measured with GaAs TUNNETT diodes around 100 GHz [40]. Fig. 12 also confirms the well-known low-noise properties of Gunn devices.

VIII. Conclusion

The power-generation capabilities of selected two-terminal devices were reviewed, and an overview of results from current research in this area was presented. It is evident from these exemplary results that significant RF power levels and low-noise performance in oscillators can be achieved with two-terminal devices operating at millimeter-wave frequencies. These devices will continue to be useful in several system applications where high power for transmitters or low noise for local oscillators is required. Improved performance such as operation at much higher millimeter-wave frequencies of TED's or much higher RF power levels in transit-time diodes from new materials can be expected as results of future research.

References

[1] P. P. Huang, T.-W. Huang, H. Wang, E. W. Lin, Y. Shu, S. D. Gee, R. Lai, H. M. Biedenbender, and J. H. Elliott, "A 94-GHz 0.35-W power amplifier module," *IEEE Trans. Microwave Theory Tech.*, vol. 45, pp. 2418–2423, Dec. 1997.

[2] Y. Hwang, J. Lester, G. Schreyer, G. Zell, S. Schrier, D. Yamauchi, G. Onak, B. Kasody, R. Kono, Y. C. Chen, and R. Lai, "60-GHz high-efficiency HEMT MMIC chip set development for high-power solid state power amplifier," in *IEEE MTT-S Int. Microwave Symp. Dig*, Denver, CO, June 17–21, 1997, pp. 1179–1182.

[3] H. Wang, R. Lai, Y. C. Chen, Y. Kok, T. W. Huang, T. Block, D. Streit, P. H. Liu, P. Siegel, and B. Allen, "A 155-GHz monolithic InP-based HEMT amplifier," in *IEEE MTT-S Int. Microwave Symp. Dig.*, Denver, CO, June 17–21, 1997, pp. 1275–1278.

[4] S. Weinreb, P. C. Chao, and W. Copp, "Full-waveguide band, 90 to 140 GHz, MMIC amplifier module," in *IEEE MTT-S Int. Microwave Symp. Dig.*, Denver, CO, June 17–21, 1997, pp. 1279–1280.

[5] O. S. A. Tang, K. H. G. Duh, S. M. J. Liu, P. M. Smith, W. F. Kopp, T. J. Rogers, and D. J. Pritchard, "A 560-mW 21% power-added efficiency V-band MMIC power amplifier," in *Proc. IEEE GaAs IC Symp.*, Orlando, FL, Nov. 3–6, 1996, pp. 115–118.

[6] H. Eisele and G. I. Haddad, "Active microwave diodes," in *Modern Semiconductor Device Physics*, S. M. Sze, Ed. New York: Wiley, 1997, ch. 6, pp. 343–407.

[7] H. Eisele, R. Kamoua, G. I. Haddad, and C. Kidner, "Active two-terminal devices as local oscillators for low-noise receiver systems at submillimeter-wave frequencies," *Arch. Elektrotech.*, vol. 77, pp. 15–19, 1994.

[8] M. Wollitzer, J. Buechler, F. Schäffler, and J.-F. Luy, "D-band Si IMPATT diodes with 300 mW CW output power at 140 GHz," *Electron. Lett.*, vol. 32, pp. 122–123, 1996.

[9] H. Eisele and G. I. Haddad, "Enhanced performance in GaAs TUNNETT diode oscillators above 100 GHz through diamond heat sinking and power combining," *IEEE Trans. Microwave Theory Tech.*, vol. 42, pp. 2498–2503, Dec. 1994.

[10] ——, "D-band InP Gunn devices with second-harmonic power extraction up to 290 GHz," *Electron. Lett.*, vol. 30, pp. 1950–1951, 1994.

[11] E. Kasper and J.-F. Luy, "State of the art and future trends in silicon IMPATT diodes for mm-wave seeker requirements," in *Proc. Military Microwaves*, London, U.K., 1990, pp. 293–298.

[12] B. Bayraktaroglu and H. D. Shih, "Integral packaging for millimeter-wave GaAs IMPATT diodes prepared by molecular beam epitaxy," *Electron. Lett.*, vol. 19, pp. 327–329, 1983.

[13] H. Eisele, "Selective etching technology for 94-GHz GaAs IMPATT diodes on diamond heat sinks," *Solid State Electron.*, vol. 32, pp. 253–257, 1989.

[14] Y. E. Ma, "Millimeter-wave active solid-state devices," *Millimeter Wave Technol. III*, vol. SPIE-544, pp. 95–102, 1985.

[15] M. G. Adlerstein and S. L. G. Chu, "GaAs IMPATT diodes for 60 GHz," *IEEE Electron Device Lett.*, vol. EDL-5, pp. 97–98, Mar. 1984.

[16] K. Akamatsu, A. Yokohata, S. Kato, N. Ohkuba, and M. Ohmori, "High-efficiency millimeter-wave GaAs Gunn diodes operating in the fundamental mode," in *Dig. 19th Int. Conf. Infrared Millimeter Waves*, Sendai, Japan, Oct. 17–20, 1994, pp. 89–90.

[17] M. Tschernitz and J. Freyer, "140 GHz GaAs double-Read IMPATT diodes," *Electron. Lett.*, vol. 31, pp. 582–583, 1995.

[18] H. Eisele and G. I. Haddad, "High-Performance InP Gunn devices for fundamental-mode operation in D-band (110–170 GHz)," *IEEE Microwave Guided Wave Lett.*, vol. 5, pp. 385–387, Nov. 1995.

[19] S. Luryi and A. Zaslavsky, "Quantum-effect and hot-electron devices," in *Modern Semiconductor Device Physics*, S. M. Sze, Ed. New York: Wiley, 1997, ch. 5, pp. 253–341.

[20] E. R. Brown, J. R. Söderström, C. D. Parker, L. J. Mahoney, K. M. Molvar, and T. C. McGill, "Oscillations up to 712 GHz in InAs/AlSb resonant tunneling diodes," *Appl. Phys. Lett.*, vol. 58, pp. 2291–2293, 1991.

[21] K. D. Stephan, S.-C. Wong, E. R. Brown, K. M. Molvar, A. R. Calawa, and M. J. Manfra, "5-mW parallel-connected resonant tunneling diode oscillator," *Electron. Lett.*, vol. 28, pp. 1411–1412, 1992.

[22] M. Reddy, S. C. Martin, A. C. Molnar, R. E. Muller, R. P. Smith, P. H. Siegel, M. J. Mondry, M. J. W. Rodwell, H. Kroemer, and S. J. Allen, "Monolithic Schottky-collector resonant tunnel diode oscillator arrays to 650 GHz," *IEEE Electron Device Lett.*, vol. 18, pp. 218–221, May 1997.

[23] E. R. Brown, C. D. Parker, A. R. Calawa, M. J. Manfra, and K. M. Molvar, "A quasi-optical resonant-tunneling-diode oscillator operating above 200 GHz," *IEEE Trans. Microwave Theory Tech.*, vol. 41, pp. 720–722, Apr. 1993.

[24] R. Blundell, D. C. Papa, E. R. Brown, and C. D. Parker, "Resonant tunneling diode as an alternative LO for SIS receiver applications," *Electron. Lett.*, vol. 29, pp. 288–290, 1993.

[25] S. M. Sze, *Physics of Semiconductor Devices*, 2nd ed. New York: Wiley, 1981.

[26] L. Wandinger, "mm-Wave InP Gunn devices: Status and trends," *Microwave J.*, vol. 24, no. 3, pp. 71–78, 1981.

[27] B. Fank, J. Crowley, D. Tringali, and L. Wandinger, "Basics and recent applications of high-efficiency millimeter wave InP Gunn diodes," in *Proc. 1st Int. Conf. Indium Phosphide Related Materials Advanced Electron. Opt. Devices*, SPIE 1144, Norman, OK, Mar. 20–23, 1989, pp. 534–546.

[28] I. Dale, J. R. P. Stephens, and J. Bird, "Fundamental-mode graded-gap Gunn diode operation at 77 and 84 GHz," in *Proc. Microwaves Conf.*, London, U.K., Oct. 25–27, 1994, pp. 248–251.

[29] S. J. J. Teng and R. E. Goldwasser, "High-performance second-harmonic operation W-band Gunn devices," *IEEE Electron Device Lett.*, vol. 10, pp. 412–414, Sept. 1989.

[30] A. Rydberg, "High efficiency and output power from second- and third-harmonic millimeter-wave InP-TED oscillators at frequencies above 170 GHz," *IEEE Electron Device Lett.*, vol. 11, pp. 439–441, Oct. 1990.

[31] K. Chang and C. Sun, "Millimeter-wave power-combining techniques," *IEEE Trans. Microwave Theory Tech.*, vol. 31, pp. 91–107, Feb. 1983.

[32] H. Eisele and G. I. Haddad, "Efficient power combining with D-band (110–170 GHz) InP Gunn devices in fundamental-mode operation," *IEEE Microwave Guided Wave Lett.*, vol. 8, pp. 24–26, Jan. 1998.

[33] M. Ino, T. Ishibashi, and M. Ohmori, "CW oscillation with p^+pn^+ silicon IMPATT diodes in 200-GHz and 300-GHz bands," *Electron. Lett.*, vol. 12, pp. 148–149, 1976.

[34] J.-F. Luy, K. M. Strohm, H.-E. Sasse, A. Schüppen, J. Buechler, M. Wollitzer, A. Gruhle, F. Schäffler, U. Guettich, and A. Klaßen, "Si/SiGe MMIC's," *IEEE Trans. Microwave Theory Tech.*, vol. 43, pp. 705–714, Apr. 1995.

[35] D. F. Peterson and D. P. Klemer, "Multiwatt IMPATT power amplification for EHF Applications," *Microwave J.*, vol. 32, no. 4, pp. 107–122, 1989.

[36] M. K. Powers, J. McClymonds, D. Vye, and T. Arthur, "Solid-state power amplifier for 61.5 GHz," *NASA Tech. Briefs*, vol. 16, no. 8, p. 31, 1992.

[37] H. Eisele, C.-C. Chen, G. O. Munns, and G. L. Haddad, "The potential of InP IMPATT diodes as high-power millimeter-wave sources: First experimental results," in *IEEE MTT-S Int. Microwave Symp. Dig.*, San Francisco, CA, June 17–21, 1996, pp. 529–532.

[38] H. Eisele and G. I. Haddad, "GaAs single-drift flat-profile IMPATT diodes for CW operation in D-band," *Electron. Lett.*, vol. 28, pp. 2176–2177, 1992.

[39] K. Kurokawa, "Noise in synchronized oscillators," *IEEE Trans. Microwave Theory Tech.*, vol. MTT-16, pp. 234–240, Feb. 1968.

[40] H. Eisele and G. I. Haddad, "InP Gunn Devices and GaAs TUNNETT diodes as low-noise high-performance local oscillators in fundamental mode," in *Proc. 6th Int. Symp. Space Terahertz Technol.*, Pasadena, CA, Mar. 21–23, 1995, pp. 167–175.

Heribert Eisele received the Dipl.-Ing. and Dr.-Ing. degrees from the Technical University of Munich, Munich, Germany, in 1983 and 1989, respectively, both in electrical engineering.

From 1984 to 1990, he worked as a Research Engineer and Teaching Assistant at the Lehrstuhl für Allgemeine Elektrotechnik und Angewandte Elektronik, where he was involved in IMPATT diode technology, millimeter-wave measurements, and semiconductor material characterization. In 1990, he joined the Solid-State Electronics Laboratory, University of Michigan at Ann Arbor, where he is currently involved as an Assistant Research Scientist in numerical simulations and fabrication technologies of two-terminal devices, applications of two-terminal devices as power sources at millimeter- and submillimeter-wave frequencies, and optical transmission of microwave and millimeter-wave signals. He has authored or coauthored more than 50 technical papers in journals and conference proceedings.

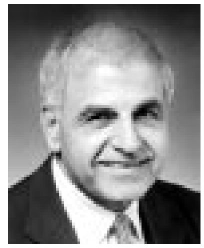

George I. Haddad (S'57–M'61–SM'66–F'72–LF'97) received the B.S.E., M.S.E., and Ph.D. degrees in electrical engineering from the University of Michigan at Ann Arbor, in 1956, 1958, and 1963, respectively.

In l958, he joined the Electron Physics Laboratory, University of Michigan at Ann Arbor, where he was engaged in research on masers, parametric amplifiers, detectors, and electron-beam devices. From 1960 to 1969, he served as Instructor, Assistant Professor, Associate Professor, and Professor in the Electrical Engineering Department. He served as Director of the Electron Physics Laboratory from 1968 to 1975. From 1975 to 1986 and 1991 to 1997, he served as Chairman of the Department of Electrical Engineering and Computer Science. From 1987 to 1990, he was Director of both the Solid-State Electronics Laboratory and the Center for High-Frequency Microelectronics. He is currently the Robert J. Hiller Professor of the Electrical Engineering and Computer Science Department and Director of the Center for High Frequency Microelectronics. His current research areas are microwave and millimeter-wave solid-state devices and monolithic integrated circuits, microwave-optical interactions, and optoelectronic devices and integrated circuits.

Dr. Haddad is a member of Eta Kappa Nu, Sigma Xi, Phi Kappa Phi, Tau Beta Pi, the American Society for Engineering Education, and the American Physical Society, and the National Academy of Engineering. He received the 1970 Curtis W. McGraw Research Award of the American Society for Engineering Education for outstanding achievements by an engineering teacher, The College of Engineering Excellence in Research Award (1985), The Distinguished Faculty Achievement Award (1986) of the University of Michigan, the S. S. Attwood Award of the College of Engineering for Outstanding Contributions to Engineering Education, Research, and Administration, and the 1996 IEEE MTT-S Distinguished Educator Award.